Langmuir

Article

pubs.acs.org/Langmuir

Ultraclean Derivatized Monodisperse Gold Nanoparticles through Laser Drop Ablation Customization of Polymorph Gold Nanostructures

Carlos J. Bueno-Alejo,[†] Claudio D'Alfonso,[†,‡] Natalia L. Pacioni,[†] María González-Béjar,[†] Michel Grenier,[†] Osvaldo Lanzalunga,[‡] Emilio Isaac Alarcon,[†] and Juan C. Scaiano*,[†]

[†]Department of Chemistry and Centre for Catalysis Research and Innovation, University of Ottawa, 10 Marie Curie, Ottawa, Ontario, Canada K1N 6N5

[‡]Dipartimento di Chimica, Sapienza Università di Roma and Istituto CNR di Metodologie Chimiche (IMC-CNR), Sezione Meccanismi di Reazione, P.le A. Moro 5, 00185 Rome, Italy

Supporting Information

ABSTRACT: We report a novel nanosecond laser ablation synthesis for spherical gold nanoparticles as small as 4 nm in only 5 s (532 nm, 0.66 J/cm^2), where the desired protecting agent can be selected in a protocol that avoids repeated sample irradiation and undesired exposure of the capping agent during ablation. This method takes advantage of the recently developed synthesis of clean unprotected polymorph and polydisperse gold nanostructures using H_2O_2 as a reducing agent. The laser drop technique provides a unique tool for delivering controlled laser doses to small drops that undergo assisted fall into a solution or suspension of the desired capping agent, yielding monodisperse custom-derivatized composite materials using a simple technique.

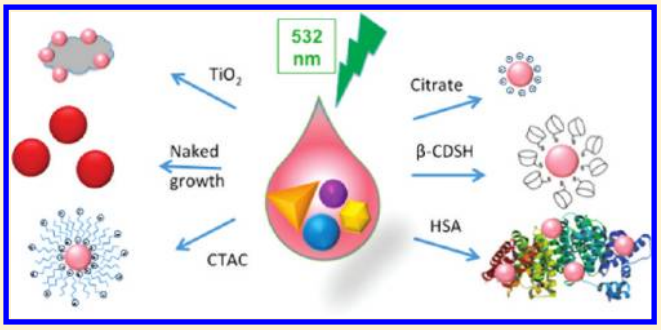

INTRODUCTION

Gold nanoparticles (AuNP) are one of the most interesting nanostructures, having found many applications in fields such as medicine,[1] sensors,[2] and catalysis.[3,4] It is generally believed that for these applications it is best to have monodisperse particles; for example, in the case of catalysis, it is generally accepted that particles with diameters ≤5 nm are most suited for this application. Some uses require clean and accessible surfaces, while others, such as sensors and medical applications, need fine control of the surface coverage with selectable coating materials. The ideal starting materials would be then a naked monodisperse nanostructure that can then be selectively modified (i.e., derivatized) for a given application. Given that the most common gold precursor for aqueous soluble colloids is $AuCl_4^-$, the strictly naked nanoparticle is probably an unrealistic goal since at least chloride is likely to be mildly associated with the nanoparticle surface. Furthermore, colloidal stability requires some overall charge on the nanoparticles. Thus, the byproduct of the reducing reagents needed to form Au(0) frequently finds its way to the surface of the nascent nanoparticle and provides the initial coverage. The removal of this coverage is difficult, frequently incomplete, and requires imaginative approaches.[5]

We have made a significant effort to prepare unprotected AuNP's with the idea that minimizing debris on the surface would intrinsically provide the best starting point for custom derivatization. In a recent article,[6] we reported several methods where all of the reagents and products involved in the reduction of $AuCl_4^-$ are easily removed or volatile.[7−9] Among these, the most interesting is the unusual application of H_2O_2 as a mild reducing agent.[9] In this case, the only byproducts of AuNP synthesis are O_2 and H_2O. This method gives the cleanest particles currently available (only Cl^- left behind); however, a lack of growth control leads to polymorph and polydisperse particles.[9]

The laser ablation of metallic materials or larger nanoparticles has also emerged as an alternative synthetic approach to the fabrication of pure metallic nanomaterials[10] or alloys.[10−12] With these techniques, however, the stabilizer must be present in the solution to prevent the formation of larger polydisperse nanoparticles. Thus, the capping agent is in direct contact with nascent nanoparticles during pulsed laser excitation, leading to the risk of stabilizer photochemical or thermal decomposition.[1] This is especially important if biomolecules (protein, aptamers, nucleic acids, and lipids) or easily oxidable molecules (i.e., thiols and amino acids) are desirable as capping agents for custom-derivatized nanocomposites.

Received: November 8, 2011
Revised: May 1, 2012
Published: May 16, 2012

dx.doi.org/10.1021/la3010689 | *Langmuir* 2012, 28, 8183−8189

In this article, we report a versatile new laser drop technique for the fabrication of monodisperse size-tunable AuNP's prepared using H_2O_2, where the protecting agent can be readily selected (i.e., citrate, thiolated cyclodextrin, cetyltrimethylammonium chloride, or human serum albumin) without compromising the integrity of the stabilizer. Furthermore, supported AuNP's (e.g., on TiO_2) can be readily prepared. This new methodology allows a remarkable level of nanoparticle surface manipulation and opens new opportunities for nanoparticle sensors, medical devices, and catalysts.

EXPERIMENTAL DETAILS

Chemicals. Gold(III) tetrachloroauric acid hydrate 99.99% ($HAuCl_4$), 50 wt % hydrogen peroxide solution, sodium citrate dihydrate (99%), albumin from human serum (HSA, lyophilized powder, fatty acid-free, globulin free, ≥99%), and 25 wt % cetyltrimethylammonium chloride solution in H_2O were obtained from Sigma-Aldrich. Nanometric titanium oxide (TiO_2, P25) was a generous gift from Evonik Degussa. In all cases, aqueous solutions were prepared using 18.2 MΩ cm^{-1} Milli-Q water at 25 °C obtained from a Millipore system (0.22 μm filter).

Synthesis and Characterization of Gold Nanoparticles (AuNP). Gold nanoparticles were prepared using a slightly modified photochemical procedure based on that described in the literature in which hydrogen peroxide is the reducing agent.[9] An aqueous solution of 10 mM H_2O_2 and 0.33 mM $HAuCl_4$ in Millipore water (treated overnight with Chelex) was irradiated in a plastic 24-well plate for 10 min using 14 UVA lamps in an LZC-L4 V photoreactor (Luzchem Research, Inc.). This method provides gold nanoparticles having a wide distribution of shapes and sizes. The AuNP's were initially characterized using UV−visible spectroscopy, revealing the presence of a broad plasmon band centered at 540 nm, and extensive light scattering at 800 nm. Nanoparticle sizes were determined using a JSM-7500F field emission scanning electron microscope (SEM) from Jeol Ltd. The samples employed in the SEM analysis were prepared by depositing 10 μL of the AuNP suspension onto a Cu grid. After a few minutes, the excess liquid was removed by using filter paper and then the grid was dried under vacuum in a desiccator overnight to remove the solvent prior to imaging. Gold nanoparticles were also characterized to determine the hydrodynamic size (HDS) of the particles by dynamic light scattering (DLS) in a Malvern Zetasizer Nano ZS at 20 °C using 1.0 cm path length disposable cuvettes, and disposable 0.5 mL folded capillary cells (from Malvern) were employed for zeta potential determinations.

Synthesis and Characterization of 6^A-Thio-β-cyclodextrin (β-CDSH). The synthesis of β-CDSH was performed in three steps according to a modified literature method.[13,14] Experimental details and NMR characterization of the precursor and final product are included in the Supporting Information (SI).

Laser Drop Technique. Laser excitation was performed with frequency-doubled 532 nm (~8 ns) pulses from a Continuum Q-switched Nd/YAG laser. The beam was concentrated in a drop generated by a computer-controlled syringe pump that delivers the sample to the exposure region through a Teflon tube having an external diameter of 1.6 mm (Figure S1). The drop volumes (typically 7−10 μL) and cross section (0.04 cm^2) were calculated by assuming spherical drops and were based on photographs taken with a Nikon D90 DSLR camera equipped with a Sigma 105 mm f 2.8 macrolens, controlled by the same software that controls the laser-drop system. In the calculation of energy fluency, we have estimated that around 52% of the laser energy goes into the drop by measuring the energy before and after a circular aperture of 2.0 mm. About 20−30% of the light is absorbed given the drop's optical path. This is probably a slight underestimate because it does not take into account internal reflections in the drop.

The irradiated drops were collected in a plastic cuvette and analyzed by UV−vis, SEM, and DLS techniques. The cuvette holds 200 μL of a stock solution of the desired stabilizer that will be diluted to a final volume of 2 mL when AuNP's are collected. A schematic diagram of the laser drop system is shown in Figure S1 (Supporting Information).

Synthesis of Gold Nanoparticles Supported on TiO_2. To prepare AuNP's on TiO_2 at 2.5% loading, we proceed as follows: 3 mL of the solution of the polymorphic AuNP was subjected to ablation by the laser drop technique as described above. Then, a suspension of 10 mg of nanometric P25-TiO_2 in 1 mL of stirred Millipore water was placed in a plastic cuvette to collect the drops. When the volume reached 4 mL, the suspension was allowed to decant for 3 h at room temperature and the supernatant was discarded. The resulting solid was washed with water and centrifuged (3600 rpm for 30 min). This process was repeated three times, leading to a solid submitted to lyophilization for 14 h in a Labconco Freezone 4.5 lyophilizer.

RESULTS AND DISCUSSION

The laser-drop technique developed in our laboratories[6,15−17] was employed to ablate polydisperse gold nanostructures formed after the photolysis of $AuCl_4^-$ in the presence of H_2O_2[9] (Figure 1). The particles were then excited at 532 nm

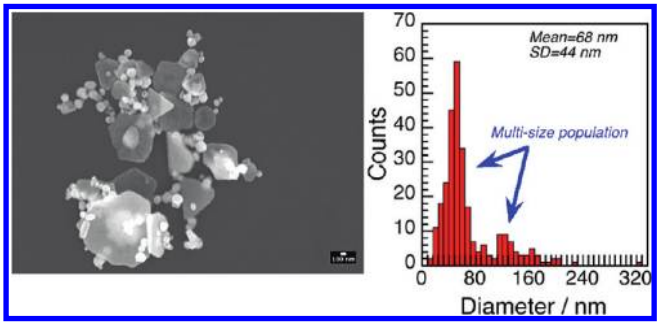

Figure 1. Representative SEM image (operating in SEI mode) for AuNP (left) prepared in the presence of H_2O_2. A histogram size analysis has been included (right).

(at the plasmon band for spherical particles) with the pulses from a frequency-doubled Nd:YAG nanosecond laser. The drops, typically ~10 μL (delivered by a syringe pump), were exposed to a number of concentrated but not focused 532 nm laser pulses operated at a frequency of 1 Hz (Figures S1 and S2 Supporting Information). Our setup allows us to control the number of pulses, the energy per pulse, and the total energy delivered to each drop.

After the desired energy has been delivered, the drop is mechanically forced to fall into a receiving cuvette that can contain a solution of the preferred capping agent or support (Figure S1). The overall process for collecting the freshly ablated nanoparticles in a solution of the desired protecting agent is schematically illustrated in Figure 2 (top), along with a series of still photographs showing the drop as it is exposed to the laser beam (bottom). Importantly, these solutions, initially yellow iridescent, clear instantly as the laser excites them (a 19 s video is included in the Supporting Information); this is fully consistent with the spectroscopic observations shown below.

We note that the delay between the last laser pulse exposure at the sample and contact with the derivatizing agent is less than 1 s in all cases. The effect of laser excitation in the absence of a protecting agent is shown in Figure 3, where the average particle size decreased from 68 ± 44 nm (Figure 1) to 12 ± 2.5 nm. Beyond the particle size, changes due to laser exposure change the nanostructure from a highly polymorphic sample (note the multiple shapes in Figure 1) to essentially spherical, nearly monodisperse, small AuNP's. Laser excitation of the polydisperse and polymorph particles has a distinct effect on

dx.doi.org/10.1021/la3010689 | Langmuir 2012, 28, 8183−8189

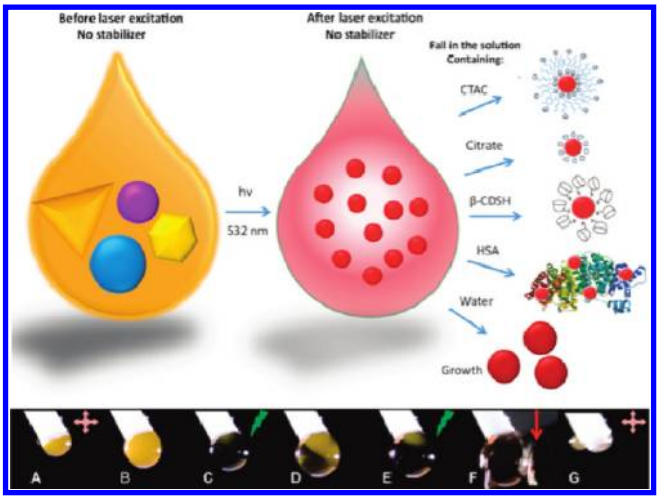

Figure 2. (Top) Schematic representation of the AuNP ablation size reduction achieved by laser ablation from the generated drop shown below. (Bottom) Still photographs exported from a video clip (24 frames/s) of laser drop ablation (clip available as Supporting Information): (A) drop growth, (B) full size of drop, (C) instant bleaching as the laser hits the drop, (D) diffusion from tube bringing some iridescent material into drop, (E) laser hitting the drop, (F) assisted drop fall, and (G) a new drop starting to form.

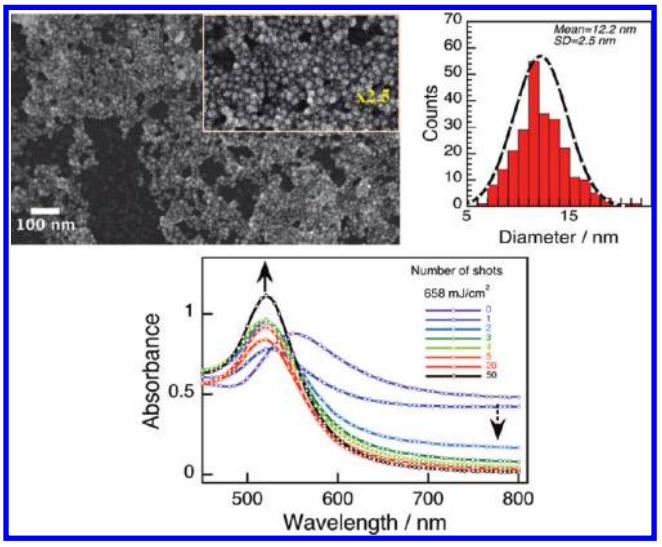

Figure 3. Effect of 532 nm Nd:YAG laser drop ablation on colloidal AuNP's prepared using H_2O_2 (top). The SEM picture (and ×2.5 enlargement) was obtained after five laser shots at 658 mJ/cm^2; the histogram analysis is included (right). Effect of the number of laser pulses on the absorption spectra of AuNP colloidal solutions from 0 to 50 pulses per drop as the arrows indicate (bottom).

the spectroscopy of the particles, as illustrated in Figure 3 (bottom); note how the absorbance in the red region ($\lambda > 600$ nm) decreases dramatically after just two pulses, indicating the removal of the larger particles that scatter more light, accompanied by an increase and narrowing of the plasmon band at ~530 nm. Overall, this effect is due to the conversion of the polymorphic AuNP's into spherical particles with excellent monodispersity as shown in the histogram in Figure 3.

We were also interested in understanding to what extent the form of energy delivery was important; therefore, we delivered a total of ~3950 mJ/cm^2 per drop but changed the form of delivery from 84 to 658 mJ/cm^2 per pulse (Table S1) while maintaining the repetition rate at 1 Hz. We concluded that a total delivered energy of 3950 ± 50 mJ/cm^2 per drop leads to particles of approximately 15 nm (if not derivatized) throughout most of the energy range (similar conclusions to those in Figure 4 were obtained from SEM imaging), with the

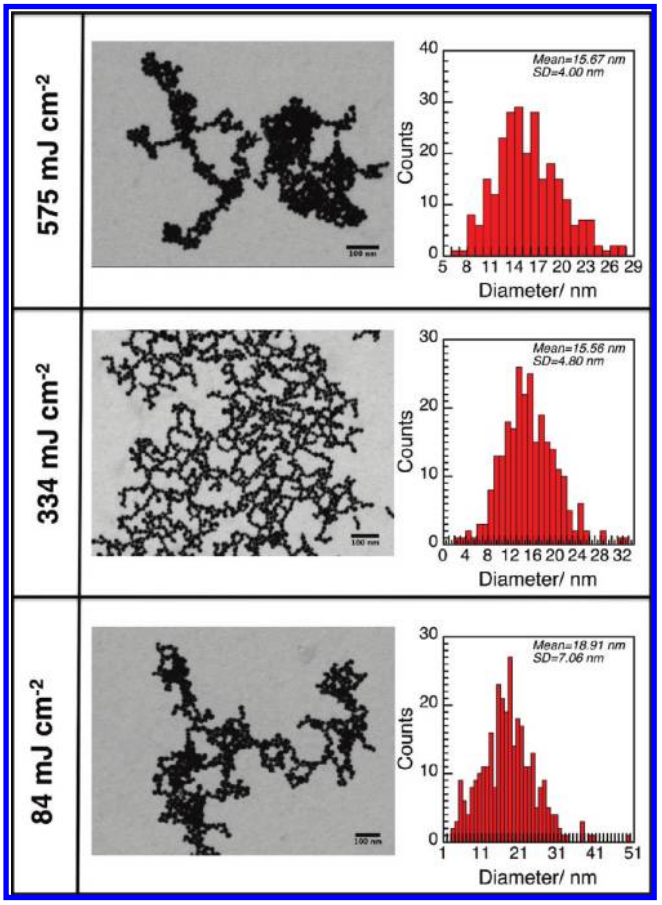

Figure 4. Nanoparticle sizes after ablation obtained using the same total energy fluency dose (3950 ± 50 mJ/cm^2) delivered through different laser energies of 575 mJ/cm^2 (7 shots, top), 334 mJ/cm^2 (12 shots, middle), and 84 mJ/cm^2 (48 shots, bottom). Nanoparticle diameter calculated from the average of at least 250 individual particles as indicated in each histogram analysis.

exception of the highest pulse energy where the size is ~12 nm (Figure 3). We note that a pulsed laser is in fact required, and continuous sources at the same wavelength (such as LEDs) do not lead to the dramatic effects reported here (data not shown). Although a low threshold for laser pulse energy must exist, we believe that this will be very dependent on the detailed experimental conditions in each laboratory (laser focus, drop size, exposure time); in our case, we have found that 49−84 mJ/cm^2 per pulse is the lowest energy that leads to dramatic size reductions.

Most of the currently available laser ablation techniques require a protecting agent from the very beginning, as is usual for the processes in Table S2. In fact, the only exception that we have found is the report by Kawasaki and Masuda on the ablation of water-suspended Au flakes (100−200 nm), where they obtained 10 nm AuNP's (details in Table S2); however, the particles were not stable in air.[18] Table S2 in the Supporting Information also shows a number of different examples of pulsed laser wavelengths (from 266 to 1064 nm) that have been

dx.doi.org/10.1021/la3010689 | Langmuir 2012, 28, 8183−8189

Table 1. Effect of Different Stabilizing Agents on Ablated AuNP (3290 mJ/cm^2) Using 658 mJ/cm^2 per Laser Pulse

sample	zeta/mV	HDS/nm	SEM/nm[b]
AuNP (no laser)	−29 ± 1.1	73 ± 1.8	70 ± 50[d]
AuNP (naked)	−22 ± 0.73	11 ± 0.59	12 ± 2.5
AuNP/citrate (1.0 mM)	−45 ± 0.15 (−51 ± 2.9)[a]	4.7 ± 1.9 (4.1 ± 0.36)	7.0 ± 2.7[e,f]
AuNP/SH-CD (0.01 mM)	−42 ± 2.1	7.5 ± 2.4	3.8 ± 1.6[f]
AuNP/CTAC (0.5 mM)	+58 ± 2.5	11 ± 1.1[c]	6.5 ± 3.0[f]
AuNP/HSA (0.01 mM)	+29 ± 0.6	31 ± 18	
2.5% AuNP/TiO_2			7.9 ± 4.0[g]

[a]Values in brackets correspond to the data collected by using 32 900 mJ/cm^2 as the total energy dose. [b]Nanoparticle diameter calculated from the average of at least 250 individual particles (Figures 3 and 6). [c]Data measured using 0.1 mM CTAC. [d]Particles with high polydispersity and different shapes. [e]Data obtained with a 0.01 mM solution. [f]Similar sizes (less than 10% difference) were obtained for all of the different concentrations employed here, from 0.01 to 1.0 mM . [g]Nanoparticle diameter calculated from the average of 60 individual particles from TEM images (Figure 7).

employed as excitation sources for the modification of metallic AuNP's in solution. Furthermore, the laser pulse duration directly controls the dominant mechanism for nanoparticle ablation. Even though any discussion of this topic is beyond the scope of the present work, it is worth noting that femtosecond, and most likely picosecond, lasers lead to particle fragmentation, also called Coulomb explosion, whereas nanosecond sources mainly operate through surface evaporation as recently described by Werner and Hashimoto.[19] In their work, they have found that a surface evaporation mechanism takes place in the regime of nanosecond excitation because of the combination of two phenomena: (i) electron−phonon coupling time > phonon−phonon coupling > laser pulse duration and (ii) quasi-thermal equilibrium for the electron and lattice temperature. Thus, these two combined conditions are responsible for the nanoparticle's size reduction through the evaporation mechanism because the boiling temperature is easily reached with a negligible contribution of fragmentation as a result of the fact that the Rayleigh instability (a critical Coulombic repulsion resulting from ejection upon laser excitation) is never reached. Table 1 also shows that there is no correlation between the final AuNP sizes and either the energy delivered to the sample or the total exposure time. In fact, the final AuNP size seems to be more closely related to the nature of the capping agent than to any other factor.[20]

We have also included our work in Table S2; it is the only one that allows the selection of the capping agent without exposing it to light during ablation, forming spherical monodisperse AuNP's in ≤5 s (Table S2). We have determined an upper production limit for unprotected 12 nm AuNP's of 7.2 mL/h for a 6.03 nM solution in AuNP's using the maximum absorption at SPB calculated according to Liu et al.[21] This number is equivalent to ∼0.46 mg Au/h, a value close to those reported using other ablation procedures for metallic films.[22]

Sizes determined by SEM are normally smaller than those measured by dynamic light scattering; the later reflects not only the metallic core but also the surface-covering materials. The only exceptions are the "naked" AuNP's, where the size is almost the same by both methods, which is another indication of the absence of stabilizers. We note, however, that these small, naked particles with a low zeta potential have a tendency to continue growing, as shown in the time evolution of the absorption spectra of Figure 5.[23] Similar results have been reported by Mufane et al.[24] for the growth of small AuNP's or metallic clusters in the dark obtained from the ablation of 8.0 nm SDS-stabilized AuNP's (532 nm, 560 mJ/cm^2 per pulse for 50 min). However, in our case the addition of citrate after 30 min as a free capping agent halts the changes in absorption at

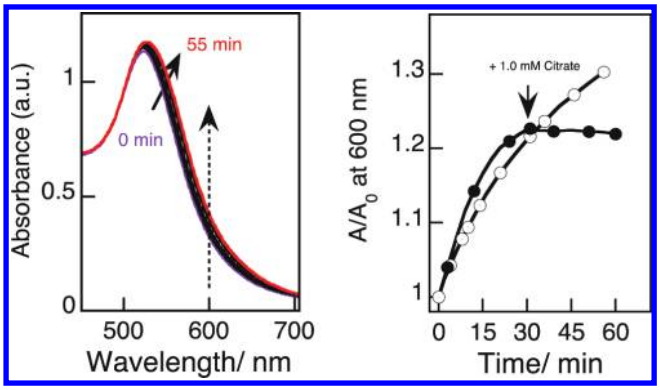

Figure 5. Absorption evolution from 0 to 55 min for ablated AuNP's with 658 mJ/cm^2 per pulse (six shots) in the absence of stabilizer (left panel). Changes in the 600 nm absorption of ablated AuNP in the absence of any stabilizer (○) and after addition at 30 min of 1.0 mM sodium citrate as indicated by the arrow in the plot (●, right panel). All measurements were carried out at room temperature.

600 nm (Figure 5). This data indicates that citrate effectively increases their colloidal stability by preventing further particle growth.

Table 1 also shows that the smallest SEM size, 3.8 nm, was obtained for particles derivatized with SH-modified cyclodextrin (Figure 6) and probably reflects the actual particle size as the ablated AuNP initially contacts the stabilizer. However, when SH-modified cyclodextrin was added to an ablated AuNP after 30 min, the nanoparticle diameter was close to 12 nm, illustrating that the AuNP size distribution could be modulated by chainging the time when the stabilizer is added. When unprotected AuNP's are exposed to a cationic surfactant such as CTAC, at concentrations below the cmc, the zeta potential was positive; this is attributed to the formation of a surfactant monolayer on the metallic surface (Figure 2, top). Furthermore, "naked" AuNP's were also stabilized by using human serum albumin (HSA) as shown in Table 1, where the presence of the protein shifts the zeta potential to positive values and prevents the subsequent growth of ablated AuNP's. Some of these particles were prepared for catalysis studies that are not part of this article, but they were included here to illustrate the small sizes achievable by the drop-ablation method. In comparison to other laser ablation procedures where large[25,26] or small AuNP's[18,20,24,27−40] were obtained, the size or protecting agent cannot be customized with the same flexibility achieved with drop-ablation techniques. Furthermore, other ablation/derivatization techniques tend to expose the particles from ablation and the capping agents to many laser

dx.doi.org/10.1021/la3010689 | Langmuir 2012, 28, 8183−8189

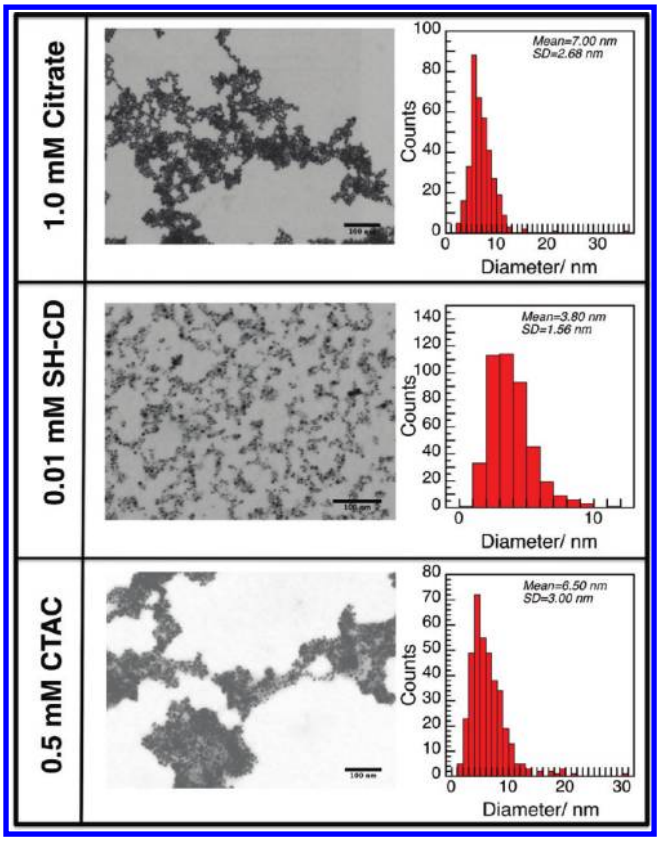

Figure 6. Selected SEM pictures and histogram analysis for the data collected in Table 1 obtained upon AuNP irradiation with 6 shots per drop at 658 mJ/cm^2 and collected in a cuvette containing 10 times the concentration of the stabilizing agent in each case. (Top to bottom) 1.0 mM citrate, 0.01 mM SH-CD, and 0.5 mM CTAC. Nanoparticle diameter calculated from the average of at least 250 individual particles.

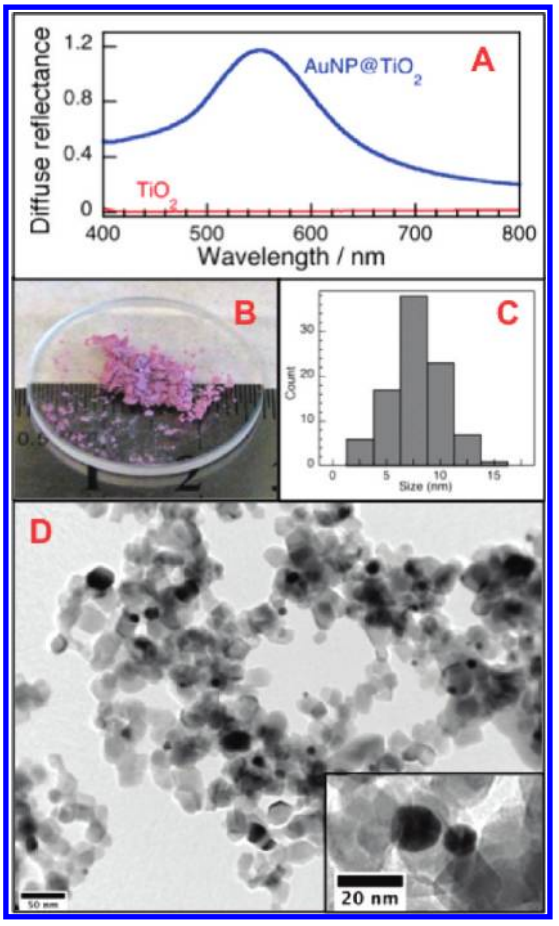

Figure 7. (A) Diffuse reflectance spectrum of AuNP@TiO_2 containing 2.5% TiO_2 prepared by the laser drop technique. (The diffuse reflectance spectrum of TiO_2 has been included for comparison.) (B) Photograph of the AuNP supported on TiO_2; the disk is 1 inch in diameter. (C) Histogram showing the size distribution of the AuNP; some of these measurements are difficult because of the limited contrast given the nanometric TiO_2. (D) TEM image of a 2.5% AuNP@TiO_2 sample; the scale bar at the bottom left is 50 nm. (E) The same as in D but for a different region of the sample showing two very well resolved small particles.

pulses until acceptable conversion is achieved; this represents a problem with capping agents such as biomacromolecules, photodegradable compounds, and easily oxidizable molecules. In contrast, the laser drop technique allows the use of almost any water-soluble molecule as the AuNP stabilizer without light exposure. Thus, we have developed a methodology allowing control of the AuNP size and capping agent using a minimum number of steps and without risking either the particle or capping agent integrity.

Supported metal nanoparticles, such as AuNP, have proven to be excellent catalysts;[41] it was therefore of interest to discover if clean ablated nanoparticles would readily deposit on common supports. To explore this possibility, we ablated AuNP, as described above, but received them in a stirred-water suspension of nanometric TiO_2. The sample in Figure 7 contains ~2.5% gold loading and shows a well-defined plasmon band at ca. 550 nm, and the TEM images (see inset) show ~8 nm AuNP. The red shift to 550 nm most likely reflects the change in the particle environment relative to that in colloidal systems.

CONCLUSIONS

Laser drop techniques enables remarkable versatility in the synthesis of custom-made, protected, spherical monodisperse AuNP's from clean, almost naked, polymorphic gold nanostructures,[9] where for the first time both the particle size and capping agent can be controlled simultaneously. This technique not only offers the possibility of modulation of the protecting agent in the solution but also can be used for the deposition of colloidal gold on the surfaces of solids supports such as TiO_2; in all cases, the particles are essentially naked (except chloride ions) as they reach the point of derivatization. This new methodology offers a convenient alternative to cleaning the particles post-synthesis.[5] In a sense, it is simpler to work with particles that never had organic matter on the surface rather than removing chemical debris.

ASSOCIATED CONTENT

Supporting Information

Schematic representation of the setup for the laser-drop experiments. Picture of the actual setup for the laser drop experiments. Effect of laser energy on the nanoparticle zeta potential and hydrodynamic size. Video clip showing the laser excitation of microdrops of nanoparticle solutions. Literature data on nanoparticle synthesis and modification using ablation techniques. This material is available free of charge via the Internet at http://pubs.acs.org.

dx.doi.org/10.1021/la3010689 | *Langmuir* 2012, 28, 8183−8189

AUTHOR INFORMATION

Corresponding Author

*E-mail: tito@photo.chem.uottawa.ca.

Notes

The authors declare no competing financial interest.

ACKNOWLEDGMENTS

We acknowledge generous financial support from the Natural Sciences and Engineering Research Council of Canada, the Canadian Foundation for Innovation, and the Canada Research Chairs program as well as Becas Chile for a postdoctoral fellowship to E.I.A. We especially thank Professor Julia Perez-Prieto (ICMOL, University of Valencia, Spain) and Professor Fumitaka Mafune (University of Tokyo, Japan) for providing valuable experimental details for Table S2. We also thank Professor James Harden (University of Ottawa) for the use of the lyophilizer in the preparation of AuNP@TiO_2.

REFERENCES

(1) Ben-Yakar, A.; Eversole, D.; Ekici, O. Spherical and Anisotropic Gold Nanomaterials in Plasmonic Laser Phototherapy of Cancer. In *Non-Magnetic Metallic Nanomaterials for Life Sciences*; Kumar, C., Ed.; John Wiley & Sons: New York, 2008; pp 493−539.

(2) Jain, P. K.; Huang, X.; El-Sayed, I. H.; El-Sayed, M. A. Noble metals on the nanoscale: optical and photothermal properties and some applications in imaging, sensing, biology, and medicine. *Acc. Chem. Res.* **2008**, *41*, 1578−1586.

(3) Grisel, R.; Weststrate, K.-J.; Gluhoi, A.; Nieuwenhuys, B. E. Catalysis by gold nanoparticles. *Gold Bull.* **2002**, *35*, 39−45.

(4) Corma, A.; Garcia, H. Supported gold nanoparticles as catalysts for organic reactions. *Chem. Soc. Rev.* **2008**, *37*, 2096−2126.

(5) Lopez-Sanchez, J. A.; Dimitratos, N.; Hammond, C.; Brett, G. L.; Kesavan, L.; White, S.; Miedziak, P.; Tiruvalam, R.; Jenkins, R. L.; Carley, A. F.; Knight, D.; Kiely, C. J.; Hutchings, G. J. Facile removal of stabilizer-ligands from supported gold nanoparticles. *Nat. Chem.* **2011**, *3*, 551−556.

(6) Scaiano, J. C.; Netto-Ferreira, J. C.; Alarcon, E.; Billone, P.; Bueno Alejo, C. J.; Crites, C.-O. L.; Decan, M.; Fasciani, C.; González-Béjar, M.; Hallett-Tapley, G.; Grenier, M.; McGilvray, K. L.; Pacioni, N. L.; Pardoe, A.; René-Boisneuf, L.; Schwartz-Narbonne, R.; Silvero, M. J.; Stamplecoskie, K.; Wee, T.-S. Tuning plasmon transitions and their applications in organic photochemistry. *Pure Appl. Chem.* **2011**, *83*, 913−930.

(7) McGilvray, K. L.; Decan, M. R.; Wang, D.; Scaiano, J. C. Facile photochemical synthesis of unprotected aqueous gold nanoparticles. *J. Am. Chem. Soc.* **2006**, *128*, 15980−15981.

(8) Marin, M. L.; McGilvray, K. L.; Scaiano, J. C. Photochemical strategies for the synthesis of gold nanoparticles from Au(III) and Au(I) using photoinduced free radical generation. *J. Am. Chem. Soc.* **2008**, *130*, 16572−16584.

(9) McGilvray, K. L.; Granger, J.; Correia, M.; Banks, J. T.; Scaiano, J. C. Opportunistic use of tetrachloroaurate photolysis in the generation of reductive species for the production of gold nanostructures. *Phys. Chem. Chem. Phys.* **2011**, *13*, 11914−11918.

(10) Boyer, P.; Ménard, D.; Meunier, M. Nanoclustered Co/Au particles fabricated by femtosecond laser fragmentation in liquids. *J. Phys. Chem. C* **2010**, *114*, 13497−13500.

(11) Izgaliev, A. T.; Simakin, A. V.; Shafeev, G. A. Formation of the alloy of Au and Ag nanoparticles upon laser irradiation of the mixture of their colloidal solutions. *Quantum Electron.* **2004**, *34*, 47−50.

(12) Peng, Z.; Spliethoff, B.; Tesche, B.; Walther, T.; Kleinermanns, K. Laser-assisted synthesis of Au-Ag alloy nanoparticles in solution. *J. Phys. Chem. B* **2006**, *110*, 2549−2554.

(13) Trotta, F.; Martina, K.; Robaldo, B.; Barge, A.; Cravotto, G. Recent advances in the synthesis of cyclodextrin derivatives under microwaves and power ultrasound. *J. Incl. Phenom. Macrocycl. Chem.* **2007**, *57*, 3−7.

(14) Martina, K.; Trotta, F.; Robaldo, B.; Belliardi, N.; Jicsinszky, L.; Cavotto, G. Efficient regioselective functionalizations of cyclodextrins carried out under microwaves or power ultrasound. *Tetrahedron Lett.* **2007**, *48*, 9185−9189.

(15) Banks, J. T.; Scaiano, J. C. The laser-drop method: a new approach to induce multiple photon chemistry with pulsed lasers. Examples involving reactions of diphenylmethyl and cumyloxyl radicals. *J. Am. Chem. Soc.* **1993**, *115*, 6409−6413.

(16) Banks, J. T.; Garcia, H.; Miranda, M. A.; Perez-Prieto, J.; Scaiano, J. C. Laser flash, laser-drop, and preparative photochemistry of 1,5-diiodo-1,5-diphenylpentane. detection of a hypervalent iodine radical intermediate. *J. Am. Chem. Soc.* **1995**, *117*, 5049−5054.

(17) Hallett-Tapley, G. L.; Silvero, M. J.; Gonzalez-Bejar, M.; Grenier, M.; Netto-Ferreira, J. C.; Scaiano, J. C. Plasmon-mediated catalytic oxidation of sec-phenethyl and benzyl alcohols. *J. Phys. Chem. C* **2011**, *115*, 10784−10790.

(18) Kawasaki, M.; Masuda, K. Laser fragmentation of water-suspended gold flakes via spherical submicroparticles to fine nanoparticles. *J. Phys. Chem. B* **2005**, *109*, 9379−9388.

(19) Werner, D.; Hashimoto, S. Improved working model for interpreting the excitation wavelength- and fluence-dependent response in pulsed laser-induced size reduction of aqueous gold nanoparticles. *J. Phys. Chem. C* **2011**, *115*, 5063−5072.

(20) Besner, S.; Kabashin, A. V.; Meunier, M. Fragmentation of colloidal nanoparticles by femtosecond laser-induced supercontinuum generation. *Appl. Phys. Lett.* **2006**, *89*, 233122−233123.

(21) Liu, X.; Atwater, M.; Wang, J.; Huo, Q. Extinction coefficient of gold nanoparticles with different sizes and different capping ligands. *Colloids Surf., B* **2007**, *58*, 3−7.

(22) Li, L.; Hong, M.; Schmidt, M.; Zhong, M.; Malshe, A.; Huis in't Veld, B.; Kovalenko, V. Laser nano-manufacturing-State of the art and challenges. *CIRP Ann. Man. Technol.* **2011**, *60*, 735−755.

(23) Kamat, P. V. Photophysical, photochemical and photocatalytic aspects of metal nanoparticles. *J. Phys. Chem. B* **2002**, *106*, 7729−7744.

(24) Mafune, F.; Kohno, J.-y.; Takeda, Y.; Kondow, T. Dissociation and aggregation of gold nanoparticles under laser irradiation. *J. Phys. Chem. B* **2001**, *105*, 9050−9056.

(25) Niidome, Y.; Hori, A.; Sato, T.; Yamada, S. Enormous size growth of thiol-passivated gold nanoparticles induced by near-IR laser light. *Chem. Lett.* **2000**, *29*, 310−311.

(26) Pocovi-Martinez, S.; Parreno-Romero, M.; Agouram, S.; Perez-Prieto, J. Controlled UV-C light-induced fusion of thiol-passivated gold nanoparticles. *Langmuir* **2011**, *27*, 5234−5241.

(27) Peng, Z.; Walther, T.; Kleinermanns, K. Photofragmentation of phase-transferred gold nanoparticles by intense pulsed laser light. *J. Phys. Chem. B* **2005**, *109*, 15735−15740.

(28) Takami, A.; Kurita, H.; Koda, S. Laser-induced size reduction of noble metal particles. *J. Phys. Chem. B* **1999**, *103*, 1226−1232.

(29) Link, S.; Burda, C.; Mohamed, M. B.; Nikoobakht, B.; El-Sayed, M. A. Laser photothermal melting and fragmentation of gold nanorods: energy and laser pulse-width dependence. *J. Phys. Chem. A* **1999**, *103*, 1165−1170.

(30) Link, S.; Burda, C.; Nikoobakht, B.; El-Sayed, M. A. Laser-induced shape changes of colloidal gold nanorods using femtosecond and nanosecond laser pulses. *J. Phys. Chem. B* **2000**, *104*, 6152−6163.

(31) Inasawa, S.; Sugiyama, M.; Noda, S.; Yamaguchi, Y. Spectroscopic study of laser-induced phase transition of gold nanoparticles on nanosecond time scales and longer. *J. Phys. Chem. B* **2006**, *110*, 3114−3119.

(32) Inasawa, S.; Sugiyama, M.; Yamaguchi, Y. Laser-induced shape transformation of gold nanoparticles below the melting point: the effect of surface melting. *J. Phys. Chem. B* **2005**, *109*, 3104−3111.

(33) Mafune, F.; Kohno, J.-y.; Takeda, Y.; Kondow, T. Full physical preparation of size-selected gold nanoparticles in solution: Laser ablation and laser-induced size control. *J. Phys. Chem. B* **2002**, *106*, 7575−7577.

(34) Yamada, K.; Tokumoto, Y.; Nagata, T.; Mafune, F. Mechanism of laser-induced size-reduction of gold nanoparticles as studied by nanosecond transient absorption spectroscopy. *J. Phys. Chem. B* **2006**, *110*, 11751−11756.
(35) Chang, S.-S.; Shih, C.-W.; Chen, C.-D.; Lai, W.-C.; Wang, C. R. C. The shape transition of gold nanorods. *Langmuir* **1999**, *15*, 701−709.
(36) Kurita, H.; Takami, A.; Koda, S. Size reduction of gold particles in aqueous solution by pulsed laser irradiation. *Appl. Phys. Lett.* **1998**, *72*, 789−791.
(37) Fujiwara, H.; Yanagida, S.; Kamat, P. V. Visible laser induced fusion and fragmentation of thionicotinamide-capped gold nanoparticles. *J. Phys. Chem. B* **1999**, *103*, 2589−2591.
(38) Takahashi, H.; Niidome, Y.; Sato, T.; Yamada, S. Effects of capping thiols on the laser-induced fusion of gold nanoparticles and deposition onto glass substrates in cyclohexane. *Colloids Surf., A* **2004**, *247*, 105−113.
(39) Giorgetti, E.; Giammanco, F.; Marsili, P.; Giusti, A. Effect of picosecond postirradiation on colloidal suspensions of differently capped AuNPs. *J. Phys. Chem. C* **2011**, *115*, 5011−5020.
(40) Giusti, A.; Giorgetti, E.; Laza, S.; Marsili, P.; Giammanco, F. Multiphoton fragmentation of PAMAM G5-capped gold nanoparticles induced by picosecond laser irradiation at 532 nm. *J. Phys. Chem. C* **2007**, *111*, 14984−14991.
(41) Corma, A.; Juarez, R.; Boronat, M.; Sanchez, F.; Iglesias, M.; Garcia, H. Gold catalyzes the Sonogashira coupling reaction without the requirement of palladium impurities. *Chem. Commun.* **2011**, *47*, 1446−1448.